

AD-A122 886

FREQUENCY DOMAIN OPTICAL STORAGE(U) IBM RESEARCH LAB
SAN JOSE CA G C BJORKLUND ET AL. 20 DEC 82 TR-1
N00014-81-C-0165

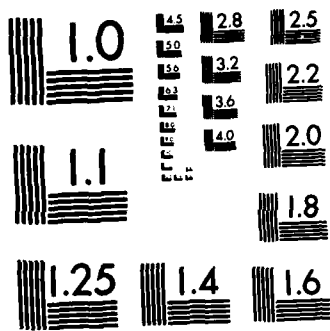
171

UNCLASSIFIED

F/G 20/6

NL

END
FILMED
DTIC



MICROCOPY RESOLUTION TEST CHART
NATIONAL BUREAU OF STANDARDS-1963-A

REPORT DOCUMENTATION PAGE

READ INSTRUCTIONS
BEFORE COMPLETING FORM

1. REPORT NUMBER 1		2. GOVT ACCESSION NO. AD-A122886		3. RECIPIENT'S CATALOG NUMBER	
4. TITLE (and Subtitle) Frequency Domain Optical Storage		5. TYPE OF REPORT & PERIOD COVERED Technical Report		6. PERFORMING ORG. REPORT NUMBER	
7. AUTHOR(s) Gary C. Bjorklund George Castro		8. CONTRACT OR GRANT NUMBER(s) N00014-81-C-0165		9. MONITORING AGENCY NAME & ADDRESS (if different from Controlling Office)	
10. PERFORMING ORGANIZATION NAME AND ADDRESS International Businesss Machines, Dept. K46 5600 Cottle Road San Jose, California 95193		11. PROGRAM ELEMENT, PROJECT, TASK AREA & WORK UNIT NUMBERS NR 421-001		12. REPORT DATE December 20, 1982	
13. CONTROLLING OFFICE NAME AND ADDRESS Office of Naval Research 800 N. Quincy Street Arlington, VA 22217 Code 240		14. NUMBER OF PAGES 34		15. SECURITY CLASS. (of this report) Unclassified	
16. DISTRIBUTION STATEMENT (of this Report) This document has been approved for public release and sale; its distribution is unlimited.		17. DISTRIBUTION STATEMENT (of the abstract entered in Block 20, if different from Report)		15a. DECLASSIFICATION/DOWNGRADING SCHEDULE	
18. SUPPLEMENTARY NOTES To be published as a book chapter.		19. KEY WORDS (Continue on reverse side if necessary and identify by block number) Optical storage, optical memories, cryogenics, tunable laser, photochemistry		20. ABSTRACT (Continue on reverse side if necessary and identify by block number) The phenomenon of photochemical hole burning makes it possible to utilize optical frequency as an additional dimension for the organization of an optical data store. Storage densities of 10^{11} bits/cm ² may ultimately be achieved. The basic principles of photochemical hole burning are reviewed in this paper and recent research results are presented.	

AD A 122886

DDIC FILE COPY

DTIC
SELECT
JAN 3 1983

DD FORM 1473 JAN 73

EDITION OF 1 NOV 65 IS OBSOLETE
S/N 0102-LF-014-5501

OFFICE OF NAVAL RESEARCH

Contract N00014-81-C-0165

Task No. NR 421-001

TECHNICAL REPORT NO. 1

Frequency Domain Optical Storage

by

Gary C. Bjorklund and George Castro

Prepared for Publication

as a Book Chapter

IBM Research Laboratory
San Jose, California 95193

December 20, 1982

Reproduction in whole or in part is permitted for
any purpose of the United States Government

This document has been approved for public release
and sale; its distribution is unlimited

FREQUENCY DOMAIN OPTICAL STORAGE

G. C. Bjorklund and G. Castro

IBM Research Laboratory
San Jose, California, 95193

- I. Introduction - Frequency Multiplexing with Spectral Hole Burning
- II. Photochemical Hole Burning
 - A. Crystalline Host Materials
 - 1. Photoreactive Organic Molecules
 - 2. Organic Phototautomers
 - 3. Alkali halide color centers
 - B. Amorphous Host Materials
 - 1. Photoreactive Organic Molecules
 - 2. Organic Phototautomers
 - 3. Rare Earth Ions in Inorganic Glasses
- III. Temperature Dependence
- IV. Data Reading and Writing Using FM Spectroscopy
- V. PHB Memory Configuration



Accession for	
NTIS	
DTIC Tab	
Unannounced	
Justification	
By	
Distribution/	
Availability Codes	
Avail and/or	
Dist	
	A

I. Introduction - Frequency Multiplexing with Spectral Hole Burning

The spatial storage density of conventional optical recording with planar geometries is, to first order, limited by diffraction to a maximum of one bit of information per square wavelength. This density of approximately 10^8 bits/cm² is about a factor of 20 greater than present day magnetic recording and is the main driving force for its development as a technology. In this chapter we will describe a method to considerably increase the maximum storage density of optical recording by storing information in the frequency spectrum at each spatial spot. This results in a maximum storage density that is determined by the number of bits that can be stored in the frequency domain multiplied by the maximum number that can be stored in the spatial domain.

The basic concept is illustrated by analogy to conventional optical storage. In Fig. 1, a tunable laser is shown which is capable of addressing a two dimensional array of spots which can be as small as $1 \mu^2$. In conventional recording the laser frequency is fixed and the optical bits are determined by the "black" or "white" nature (ie. transmissive or reflective) of the spots. In frequency selective storage, the laser is tunable and the individual spots have an absorption spectra which contain a bit pattern in the form of narrow spectral holes or spikes which can be read by scanning the laser frequency over the spectrum at each individual spot. The phenomenon that allows the formation of such a spectral pattern is referred to as spectral hole burning, or merely hole burning*.

* This terminology is unfortunately confusing with that in conventional ablative optical recording, but it has been used by spectroscopists for over three decades.

Hole burning can be achieved in the absorption spectrum of a material when a variety of conditions are fulfilled. This is illustrated in Fig. 2, which is representative of the absorption band of a sample containing a photo-reactive species dissolved in a transparent medium. The photo-absorbing species (molecules, atoms, ions, etc.) have their optical transitions distributed over a spread of energies, W_i , centered around some mean due to the fact that although the absorbers are identical, they each experience a slightly different environment which affects their transition frequencies. This is called "inhomogeneous broadening" due to the inhomogeneous nature of the absorbers environment and is found in the spectrum of all real materials. Inhomogeneous bands usually have a Gaussian shape. The narrow linewidth of each individual absorber which collectively make up the inhomogeneous band is called the "homogeneous" or "natural" linewidth, W_h , and is determined by all the processes by which the excited state of the individual absorber is relaxed. Homogeneous linewidths have a Lorentzian lineshape. Excitation with a narrow frequency laser results in absorption by only a subset of absorbers whose environment allows them to be resonant with the laser frequency. If after absorption those excited species lose their ability to absorb light at that laser frequency by some suitable chemical transformation, a dip or hole will appear in the inhomogeneous band at the laser frequency.

The use of spectral hole burning to accomplish frequency domain storage which could be combined with spatial domain storage in optical recording was first proposed by Szabo¹. In Szabo's scheme, the holes are produced by exciting absorbers to an excited electronic state which ultimately relaxes back to the ground state. In this case, the information storage is "volatile" and must constantly be refreshed within the lifetime of the excited state. It may be possible that this method could be useful as a a buffer

memory in a configuration where volatility is not an issue. The method being pursued at the IBM San Jose Research Lab² involves the excitation of absorbers which subsequently undergo a chemical transformation to form permanent holes, or non-volatile storage, if the material is maintained at cryogenic temperatures. This is referred to as photochemical hole burning (PHB), and as will be detailed below, many material systems have been identified which allow the burning of as many as 10^3 holes in their absorption bands,

II. Photochemical Hole Burning (PHB)

The number of bits that can be stored in a spectrum is determined by the ratio of the inhomogenous bandwidth to the homogeneous linewidth. An ideal system would exhibit a very small homogenous width and a very large inhomogenous width. Unfortunately, in the materials investigated thus far, there appears to be a rough correlation of inhomogenous and homogenous widths such that their ratio is in the range 10^2 to 10^4 with most systems exhibiting a ratio of 10^3 . The criteria that are necessary for the occurrence of narrow holes (apart from the necessity of cryogenic temperatures which is discussed below) have been reported^{3,4} in some detail for molecular systems dissolved in organic solids. Basically, molecular absorbers are required in which the absorption is due to a pure electronic transition (zero-phonon states) and not one which involves the creation of lattice phonons or molecular vibrations in the excitation process. The latter criterion eliminates the use of most photochemicals since, almost by definition, photochemically active molecules exhibit strong coupling of the excited electronic state to chemical bonds (ie. strong electronic-vibrational coupling). As a result, their absorption spectra exhibit little or no intensity in the zero-phonon state (ie. small Franck-Condon or Debye-Waller factors). The PHB material system examples which are given below are essentially ones in which a localized absorber is dissolved in a transparent insulating solid. In general, the

spectra of dopants in semiconductors (eg. Cr in GaAs) are expected to show only broad holes, and exciton spectra are not expected to exhibit any holeburning⁵ at all. In fact, in the systems below, narrow spectral holes are only observed for dilute absorbers because resonant interactions between identical absorbers leads to a relaxation (properly referred to as a dephasing) or homogenous broadening of the excited state, resulting in broader holes.

A. Crystalline Host Materials

The inhomogeneous bandwidths of absorbers dissolved in organic and inorganic crystals are of the order of 10-300 GHz and are primarily caused by strains and dislocations in the crystal. In certain guest-host combinations, a series of discrete bands are observed that can be separated in energy by as much as 2000 GHz and these correspond to different discrete configurations of the guest in the host. This could be due to either different orientations of the guest in a given host site or in different types of host sites. In general, these different discrete bands each exhibit bandwidths of the order of 10-300 GHz at cryogenic temperatures, ca. 2-4°K.

1. The system dimethyl-s-tetrazine in durene is typical of a photoreactive molecule dissolved in an organic host crystal. DMST undergoes irreversible photodecomposition into CH_3CN and N_2 upon absorption of two photons⁴ at low temperatures. It is the two-photon nature of the photodecomposition that allows DMST to exhibit narrow PHB holes. Absorption of the first photon leads to spectral site selection, and the absorption of the second photon leads to permanent chemical change. deVries and Wiersma⁶ measured an inhomogeneous bandwidth of 7GHz and a homogenous linewidth of 24 Mhz, the latter being completely determined by the 6 nanosecond lifetime of the excited state.

2. The system free base porphyrin (H_2P) dissolved in a n-octane crystal is an example of an absorber which undergoes a tautomerization upon excitation. It is also an example of a system mentioned above that exhibits discrete bands corresponding to different configurations of the guest molecule in the host crystal. This is diagrammatically illustrated in Fig. 3. The figure shows two orientations of the guest molecule with respect to the host, resulting in two absorption bands separated by ca. 1500 GHz, with each band having an inhomogeneous width of ca. 90 GHz. Excitation into either of the bands causes the central hydrogens to tautomerize 90° into chemically equivalent positions but with a different orientation with respect to the host. Hole burning occurs because narrow band excitation converts the subset of absorbers into tautomers whose absorbing frequency is shifted into the other inhomogeneously broadened band. In this system, Voelker et. al.⁷ were able to burn 30 Mhz holes in the 90 GHz bands at ca $2^\circ K$. This is an example of a reversible system, or more appropriately a "postable" system, since the original spectrum can be regained (ie. all holes erased) although it is not possible to selectively erase individual holes.

3. Color centers in alkali halide crystals exhibit photochemical hole burning leading to spectral holes which persist for several hours at $4.2^\circ K$. The mechanism is not fully understood but evidently some orientation of the photoexcited center occurs⁸, or the electrons in the center tunnel into adjacent traps⁹. Macfarlane and Shelby⁹ observed 38 Mhz holes in an inhomogenous band of 51 GHz of the F_3^+ center in NaF at $1.8^\circ K$. Ortiz et. al.¹⁰ observed holes as narrow as 100 Mhz in ca. 60 GHz bands in the N_1 center in NaF. The centers were produced in the top few microns of the surface of the NaF crystal by electron and ion bombardment. The great advantage of alkali halide as hosts lies in the fact that the peak absorption can be varied systematically in frequency by

choice of the kind of alkali halide host. This is shown in Fig.4 for the R (3 electron center) and the N (4 electron) centers. This plot is useful for matching the materials to the wavelength range of desirable lasers such as HeNe or GaAs. This is another example of a "postable" system. Irradiation with UV light erases all of the holes, but again it is not possible to erase an individual hole.

B. Amorphous Host Materials

Amorphous host materials would appear to be more ideal candidates for optical storage due to their ease of fabrication as large area planar films. The inhomogenous bandwidths of absorbers dissolved in amorphous hosts is much larger than their crystalline counterparts. Typical values are of the order of 10^4 GHz for both organic and inorganic amorphous hosts. Unfortunately, the homogenous linewidths are also larger due to rapid dephasing processes of excited states by low frequency motions in amorphous materials which persist even at cryogenic temperatures¹¹.

1. The molecule DMST exhibits hole burning when it is incorporated in polymer matrices such as polystyrene or polyvinylcarbazole¹². At high laser intensities, this system exhibits true irreversible photochemistry as the hole burning mechanism; however, at very low laser intensities, this system exhibits hole burning due to a "photophysical" mechanism very similar to that observed for spectral hole burning in the absorption of photochemically stable molecules dissolved in organic glasses¹³. The inhomogenous bandwidth is 9×10^3 Ghz (300 cm^{-1}) at 1.8° Kelvin in the PVK host as compared to 7 Ghz in the durene crystal host mentioned above. This three order of magnitude increase in inhomogenous bandwidth is however accompanied by a similar increase in homogenous linewidth (12 GHz as compared to 23 MHz in the crystal), albeit for different but not

unrelated reasons. The linewidths are temperature dependent even at these low temperatures and in a manner identical to that found for molecules in organic glasses. These large temperature dependent linewidths have been attributed to rapid dephasing processes of electronic states in amorphous hosts due to the coupling of the electronic state to a distribution of low energy motions (ie. two-level tunneling modes) that exist in amorphous media even at very low temperatures.

2. The system metal free phthalocyanine (H_2PC) in polymethylmethacrylate (PMMA) is an example⁴ of a PHB system that undergoes phototautomerism. (H_2PC) is similar to free base porphyrin and the phototautomerism is expected to be the same kind of 90° exchange of the central protons. Figure 5. shows a 20 bit pattern of holes burned into the low energy side of the inhomogenous band. This same pattern is expanded in Figure 6. to show the excellent signal-to-noise of frequency domain storage that is achievable in this system. The homogenous linewidths are ca. 10GHz and the inhomogenous bandwidth is ca. 10^4 GHz at $4.2^\circ K$.

3. PHB has not yet been reported for absorbers (eg. rare earth ions) dissolved in amorphous inorganic hosts; however, the nearly related studies of fluorescence line narrowing¹⁴ yields information that can predict what kinds of properties these systems might exhibit. Inorganic glasses are expected to exhibit very large inhomogenous bandwidths. The fact that they can be prepared at high temperatures offers the possibility of quenching in inhomogenous environments of the order of 10^5 GHz. Systems already prepared at a few hundred degrees Kelvin have exhibited inhomogenous bandwidths (10^4 GHz) of that same order of energy (ie. $550^\circ K = 400 \text{ cm}^{-1} = 1.2 \times 10^4 \text{ Ghz}$). The inhomogenous linewidths are expected to be of the order of 1-10GHz and again the

homogenous linewidth being dominated at low temperatures by the dephasing due to the tunnelling type of motion between low energy state in amorphous media.

III. Temperature Dependence

Unfortunately, the use of PHB to store information in the frequency domain appears to be relegated to a cryogenic phenomena. The homogenous linewidths for the systems reported above broaden so rapidly with increasing temperature that they are expected to be of the same order as the inhomogenous bandwidths at room temperature. Only the crystalline host systems retain narrow spectral holes for temperatures as high as 25°K. The other systems usually show a linear to quadratic increase of hole width with temperature, such that holes are usually not observable above 30°K. It now appears that holes must be written and read at low temperatures; nevertheless, it does appear possible that systems can be found that will retain the information written into them at low temperatures even when they are warmed to room temperature. Evidence for such a possibility is given in Figure 7. which shows the effect of temperature cycling on a photochemical hole burned in H₂PC/PMMA⁴ at 4.2°K. The narrow hole burned at 4.2°K is not measurable at 80°K; but if the sample is cooled back to 4.2°K, the hole reappears. In this particular sample the hole can still be read after remaining at 80°K for several hours. At this temperature the molecule is vibrating in its cage in the host, but it only slowly escapes from its cage or configuration in the site. It settles back into its original configuration upon re-cooling. It is conceivable that a system can have such a large energy barrier between configurations that they cannot interchange even at room temperatures.

IV. Data Reading and Writing Using FM Spectroscopy

In order to effectively utilize the very large storage capacities which PHB memories offer, it is necessary to develop means for rapidly writing data into and reading data out of the memory. Both the writing and the reading speeds are limited by the time delay in accessing the desired spatial location and by the time delay encountered in tuning the laser to the desired optical frequency. In addition, the writing speed is limited by the intrinsic rate of the hole burning photochemistry, while the reading speed is limited by the dwell time necessary to detect the presence or absence of a hole with sufficient signal to noise.

The discussion of this section will be restricted to FM spectroscopy techniques for laser frequency tuning and detection of the holes. Spatial access times are considered in the next section.

The newly developed technique of FM spectroscopy uses frequency modulated (FM) laser radiation to rapidly detect weak optical absorption features.^{15,16,17} The spectral feature of interest, which in this case is a photochemical hole bleached into a broad absorption band, is probed by a single FM sideband, and the strength of the absorption or dispersion is measured by monitoring the phase and amplitude of the rf heterodyne beat signal that occurs when the FM spectrum is distorted. The advantages of FM spectroscopy are that rapid and sensitive absorption or dispersion measurements can be obtained, the narrow linewidth of the original laser source is preserved, up to 200 GHz of optical frequency can be accessed without tuning the laser, and that the hole is exposed to very low power densities.

The FM optical spectrum is obtained by passing the output of a single frequency laser through an external phase modulator driven at a rf frequency large compared to the

width of the spectral feature. As a result, the FM sidebands are widely separated, and the spectral feature can be probed with a single sideband. The sideband can be scanned through the entire lineshape by tuning either the laser frequency with the rf frequency held constant or by tuning the rf with the laser frequency held constant. Since single-mode lasers have little noise at rf frequencies, the sensitivity of the method can be shot noise limited.

Figure 8 shows a schematic of a typical experimental arrangement for FM spectroscopy. A single frequency laser provides radiation at the optical carrier frequency ω_c , and the beam is passed through a phase modulator driven by a sinusoidally varying rf field at frequency ω_m . In the limit that the modulation index $M \ll 1$, the electric field $E_2(t)$ emerging from the modulator is described by $E_2(t) = 1/2\tilde{E}_2(t) + c.c.$ where

$$\tilde{E}_2(t) = E_0 \left\{ -\frac{M}{2} \exp [i(\omega_c - \omega_m)t] + \exp[i\omega_c t] + \frac{M}{2} \exp [(\omega_c + \omega_m)t] \right\} \quad (1)$$

and E_0 is the electric field amplitude of the original laser beam. This is a pure FM optical spectrum with sidebands at frequencies $\omega_c \pm \omega_m$. Figure 9 shows the power spectrum and illustrates the case where the $\omega_c + \omega_m$ sideband probes an isolated photochemical hole.

The beam emerging from the modulator is next passed through the PHB memory recording material. The slowly varying intensity envelope, $I_3(t)$, of the transmitted beam impinging on the photodetector is given by

$$I_3(t) = \frac{cE_0^2}{8\pi} \cdot \exp [- 2\delta(\omega_c)]$$

$$\cdot \{ [\phi(\omega_c - \omega_m) - 2\phi(\omega_c) + \phi(\omega_c + \omega_m)] \sin \omega_m t \} \quad (2)$$

$$+ \{ \delta(\omega_c + \omega_m) - \delta(\omega_c - \omega_m) \} \cos \omega_m t \},$$

where $\delta(\omega)$ and $\phi(\omega)$ are, respectively, the amplitude attenuation and phase shift experienced by light at frequency ω in passing through the recording material.

The photodetector electrical signal is proportional to $I_3(t)$, and thus will contain a beat signal at the rf modulation frequency ω_m if $\delta(\omega_c + \omega_m) - \delta(\omega_c - \omega_m) \neq 0$ or if $\phi(\omega_c + \omega_m) + \phi(\omega_c - \omega_m) - 2\phi(\omega_c) \neq 0$. The in-phase ($\cos \omega_m t$) component of the beat signal is proportional to the difference in amplitude loss experienced by the upper and lower sidebands, whereas the quadrature ($\sin \omega_m t$) component is proportional to the difference between the phase shift experienced by the carrier and the average of the phase shifts experienced by the sidebands. If ω_m is small compared to the width of the hole, then the in-phase component is proportional to the derivative of the absorption, and the quadrature component is proportional to the second derivative of the dispersion. By utilizing a phase sensitive detector such as an RF mixer, a dc signal proportional to either the absorption or phase shift can be produced.

The rf beat signal arises from a heterodyning of the FM sidebands, and thus the signal strength is proportional to the geometrical mean of the intensities of one sideband and of the carrier. Thus the signal strength is proportional to $E_0^2 M$, while the intensity of the probing sideband is $I = cE_0^2 M^2 / 8\pi$. Because of the different M dependence, arbitrarily large signal strengths can be achieved for arbitrarily low sideband intensities by properly adjusting the values of E_0 and M . The perturbing effects of the probing sideband on the spectral feature can thus be minimized. The null signal that occurs when the FM spectrum is not distorted can be thought of as arising from a perfect cancellation of

the rf signal arising from the upper sideband beating against the carrier with the rf signal arising from the lower sideband beating against the carrier. The high sensitivity to the phase of amplitude changes experienced by one of the sidebands results from the disturbance of this perfect cancellation.

FM spectroscopy is sensitive to very small absorptions for two reasons. First, the heterodyne signal amplification produces a strong signal which is far above the level of internally generated photodetector noise. Second, the signal is produced at RF frequencies where single mode lasers have very little noise. Assuming unity quantum efficiency and that the only significant source of noise is shot noise, a formal analysis shows that the minimum detectable differential absorption $\Delta\delta_{\min}$, where $\Delta\delta = \delta(\omega_c + \omega_m) - \delta(\omega_c - \omega_m)$, is $\Delta\delta_{\min} = 2[M^2(P_o/\hbar\omega_c)\tau]^{-1/2}$ where the quantity $M^2(P_o/\hbar\omega_c)\tau$ is four times the number of photons in a sideband arriving over a dwell time τ . Thus for a 1 milliwatt laser with $M=0.1$ and $\tau=1$ second, $\Delta\delta_{\min} \cong 2 \times 10^{-7}$. On the other hand, if the required absorption sensitivity is less, the necessary dwell time is considerably reduced. Thus for the same laser parameters, a $\Delta\delta$ of 10^{-2} could be measured in a dwell time of $\tau=400$ picoseconds! The only other constraint is that τ be long enough for several RF cycles to occur. Since the RF modulation frequencies will typically be in the GHz range, absorptions as small as 10^{-2} could in principle be measured with nanosecond dwell times.

The ability of FM spectroscopy to rapidly detect photochemical holes has been experimentally demonstrated.¹⁷ In these experiments, an acousto-optic amplitude modulator was placed between the tunable dye laser and the phase modulator. The acousto-optic modulator was utilized to break up the FM light into trains of microsecond duration pulses with arbitrary separation and thus arbitrarily low duty factor. Scanning over the absorption profiles was accomplished by tuning the laser output frequency ω_o , and the spectra were

displayed using a storage oscilloscope. In addition, standard transmission spectra (without frequency modulation) were taken with the help of a lock-in amplifier by driving the acousto-optic modulator with a 1:1 duty cycle in order to compare FM spectroscopy to a traditional spectroscopic technique for observing photochemical holes.

Figure 10(a) shows the spectrum of an isolated photochemical hole burned into the 6070 Å zero-phase line of the N_1 color center in NaF, taken by the standard technique of measuring the intensity of the laser excited fluorescence. The laser was tuned over 5 GHz in a scan time of 250 msec and a lock-in amplifier employed for signal averaging. Figure 10(b) shows the in-phase (absorption) signal obtained by FM spectroscopy with $\omega_m = 80$ MHz and the acousto-optic modulator set to produce 5 μ sec duration laser pulses separated by 5 msec. The rf beat signal was recorded by directly feeding the output of the double balanced mixer into the storage oscilloscope which had a bandwidth of 1 MHz. No signal averaging was utilized, and the rf signal corresponding to each of the individual spots of the obtained trace in Figure 10(b) was detected in the 5 μ sec duration of the laser pulses. In this experiment, the limitations of our storage scope prevented us from demonstrating even faster detection times. However, it is clear that FM spectroscopy is capable of detecting photochemical holes at MHz data rates.

In some cases, it is desirable to utilize a fixed frequency laser and tune the sideband frequency by tuning ω_m . The amount of tuning of the probing FM sideband which can be achieved is limited by the external phase modulator. Modulation frequencies up to 50 GHz are within the state of the art (18), and thus it should be possible to achieve 3 cm^{-1} of spectral coverage with any fixed frequency laser source. Thus it appears that FM spectroscopy should be capable of covering the entire inhomogeneous absorption bands of either porphin or F_3^+ color centers without tuning the laser. Writing

of holes would be accomplished by increasing the rf drive level to put a significant fraction of the laser power in the sideband and then modulating the laser intensity as the sideband was swept through the inhomogeneous absorption band.

Even faster reading and writing speeds could be achieved using a multiplex version of FM spectroscopy. Figure 11 shows a schematic experimental arrangement. The carrier frequency ω_c would be supplied by a fixed frequency laser operating at an optical frequency near to, but not coincident with, the inhomogeneous absorption band. The external phase modulator is driven simultaneously at n different RF frequencies, $\omega_1, \omega_2, \dots, \omega_k$. Provided that $M \ll 1$ for each RF modulation frequency, M pairs of upper-end and lower FM sidebands are produced at frequencies $\omega_c \pm \omega_1, \omega_c \pm \omega_2, \dots, \omega_c \pm \omega_k$. Thus each sideband probes a separate optical frequency location. Figure 12 shows the relative frequency positions of the FM sidebands and the inhomogeneous absorption band.

Reading would be accomplished by producing weak upper FM sidebands which simultaneously probe all possible hole locations without causing significant additional hole burning. Since the lower FM sidebands are outside of the inhomogeneous absorption band, they always experience less loss than the upper FM sidebands, and thus signals are present at all RF beat frequencies. The presence or absence of a hole at a given optical frequency location would be determined by monitoring the intensity of the corresponding RF beat signal. The presence of the hole would be indicated by a small RF signal, while the absence of the hole would be indicated by a larger RF signal. Given 100 MHz spacing between the hole locations, complete reading of all of the information encoded at a specific spatial storage location could theoretically be accomplished in less than 100 nsec, since the different RF beat signals can exist simultaneously and be simultaneously

monitored using phase-sensitive multiplex analyzing electronics. If 1000 sidebands were utilized, burst reading data rates of 10^{10} bits/sec per laser beam could be achieved.

Writing would be accomplished by driving the phase modulator with intense RF fields at selected frequencies. This would produce strong simultaneous FM sidebands at the frequency locations where hole burning is desired. Only the upper FM sidebands would burn holes, since the carrier and the lower sidebands are not coincident with the inhomogeneous absorption band.

V. PHB Memory Configurations

The derivative FM spectroscopy approach illustrated in Figure 10 provides the basis for a memory configuration which is equivalent to a very large direct access storage device (DASD) system. In today's technology, DASD devices are based on inductive magnetic recording on disks.

Figure 13 shows the reading and writing timing diagram for this configuration. The laser frequency is repetitively ranged between ω_{\min} and ω_{\max} at a 30 KHz rate. Thus, every 30 μ sec, the laser is scanned over the inhomogeneous line. For writing, the effective photochemical hole burning rate is controlled by a time varying external gating voltage. This gating could be achieved, for instance, by driving a fast light gate placed in front of the recording medium or by using an external field to control the quantum yield of the hole burning process itself. For reading, the laser is FM modulated at ω_m less than or equal to the hole width and the raw derivative FM signal monitored as a function of time. The differentiation process effectively suppresses the slowly varying inhomogeneous

lineshape. Pulse shaping electronics are employed to reproduce the original data pulse shapes.

Figure 14 shows a multiple arm memory system constructed using these principles. The centralized components consist of the current tuned GaAlAs laser, the phase modulator and driver, an array of 64 photodetectors followed by double balanced mixers, an array of 64 gating drivers, and a 100 spot acousto-optic deflector for arm selection. Each arm consists of a $10^3 \times 10^3$ spot XY galvanometer driven mirror pair, a holographic optical element which acts both as a focusing lens and 64x beam multiplexer, and an array of 64 1 cm squares of recording medium. The 100 arms are contained in a cubic meter LHe cryostat.

Each 1 cm square of recording medium contains 10^6 spatial storage locations and hence $10^3 \times 10^6$ or 10^9 bits of information. Each arm thus contains 6.4×10^{10} bits, and the entire system contains 6.4×10^{12} bits. The data is organized into 6.4×10^4 bit pages, each defined to consist of 10^3 time domain bits flowing in the 64 parallel data channels. The time to react or write a page is thus 30 μ sec.

Since galvanometer driven mirrors have settle times on the order of 3 nsec, only 1% of the time for each arm is spent reading or writing data. The remaining 99% of the time is effectively dead time, while the mirrors are moving to the next position. This makes possible time sharing of the centralized components among the 100 arms to insure that data is being read or written into one of the arms at all times. Thus the average data rate is on the order of 2×10^9 bits/sec. Data erasing is most easily accomplished on an arm by arm basis using flood illumination from a UV lamp.

The multiplex FM spectroscopy approach illustrated in Figures 11 and 12 coupled with electro-optic beam deflection provides the basis for an unusual memory configuration with extremely high data rates and fast random access time, but with limited total storage capacity. Figure 15 shows the overall set-up. The output of the fixed frequency laser is passed through the phase modulator simultaneously driven at 1000 different RF frequencies. For writing, the intensity of each of the RF fields is directly controlled by the corresponding input data channel. The laser beam is next passed through a 10^6 spot electro-optic deflector with 1 μ sec random access time to each spot and focused onto a 1 cm square of recording medium. Reading is accomplished by utilizing phase sensitive multiplex electronics to analyze the photodetector output and drive the 1000 parallel data output channels.

The total memory capacity would be $10^3 \times 10^6$ or 10^9 bits of information. The data is organized into 1000 bit pages, each defined to consist of 1 time domain bit flowing in 1000 parallel data channels. The time to read or write a page is 100 nsec, corresponding to a burst data rate of 10^{10} bits/sec. The average data rate is limited by the random access time to 10^9 bits/sec.

This work was partially supported by the Office of Naval Research.

REFERENCES

1. A. Szabo, "Frequency Selective Optical Memory", U.S. Patent No. 3,896,420, (1975).
2. G. Castro, D. Haarer, R. M. Macfarlane, and H. P. Trommsdorff, "Frequency Selective Optical Data Storage Systems, U.S. Patent No. 4,101,976, (1978).
3. D. M. Burland and D. Haarer, "One and Two-Photon Laser Photochemistry in Organic Solids, IBM J. Res. Develop., 23, 534, (1979).
4. A. R. Gutierrez, J. Friedrich, D. Haarer and H. Wolfrum, "Multiple Photochemical Hole Burning in Organic Glasses and Polymers: Spectroscopy and Storage Aspects", IBM J. Res. Develop., 26(2), March, 1982.
5. An exception to this might be found in weakly coupled exciton states such as $\text{EuP}_5\text{O}_{14}$ (see R. M. Shelby and R. M. Macfarlane, Phys. Rev. Lett., 45(13), 1098, (1980).
6. H. deVries and D. A. Wiersma, Phys. Rev. Lett., 36, 91, (1976) and Chem. Phys. Lett., 51, 565, (1977); J. H. Meyling, R. P. Van der Werf and D. A. Wiersma, Chem. Phys. Lett., 28, 364, (1974).
7. S. Voelker, R. M. Macfarlane, A. Z. Genack, H. P. Trommsdorff and J. H. van der Waals, J. Chem. Phys., 67, 1759, (1977).
8. M. D. Levenson, R. M. Macfarlane and R. M. Shelby, Phys. Rev. B 22, 4915, (1980).
9. R. M. Macfarlane and R. M. Shelby, Phys. Rev. Lett., 42, 788, (1979).
10. C. Ortiz, R. M. Macfarlane, R. M. Shelby, W. Lenth and G. C. Bjorklund, Appl. Phys., 25, 37, (1981).
11. T. L. Reinecke, Solid State Commun., 32, 1103, (1979); J. M. Hayes, R. P. Stout and G. J. Small, J. Chem. Phys., 73, 4129, (1980); S. K. Lyo and R. Orbach, Phys. Rev.

- B, 22(9), 4223, (1980); J. Klafter and R. Silbey, Chem. Phys. Lett., to be published;
P. Reinecker and H. Morawitz, Chem. Phys. Lett., to be published.
12. E. Cuellar and G. Castro, Chem. Phys., 54, 217, (1981).
 13. G. J. Small, "Nonphotochemical Hole Burning", in "Molecular Spectroscopy", Vol. of the Series, Modern Problems in Solid State Physics (Agranovich and Maradudin, Eds.), North Holland Publ. Co.
 14. P. Avouris, A. Champion and M.A. El-Sayed, J. Chem. Phys., 67, 3397, (1977); J. Hegarty and W.M. Yen, Phys. Rev. Lett., 43(15), 1126, (1979); J. R. Morgan, E. P. Chock, W. D. Hopewell, M. A. El-Sayed and R. Orbach, J. Phys. Chem., 85, 747, (1981).
 15. G. C. Bjorklund, Opt. Lett. 5, 15 (1980).
 16. G. C. Bjorklund, W. Lenth, M. D. Levenson, C. Ortiz, SPIE 286, 153 (1981).
 17. W. Length, C. Ortiz, G. C. Bjorklund, Opt. Lett. 6, 35 (1981).
 18. G. M. Carter, Appl. Phys. Lett., 32, 810 (1978); G. Magerl and E. Bonek, Appl. Phys. Lett., 34, 452 (1979).

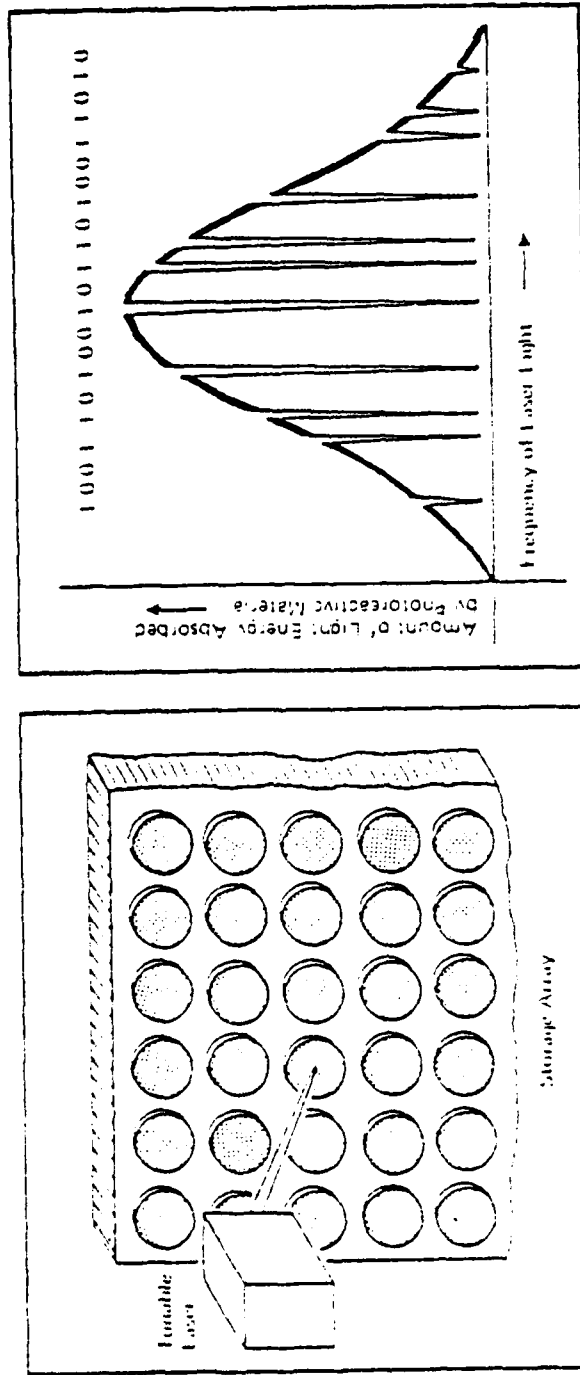


Figure 1. Schematic description of the frequency domain storage concept. The left-hand side shows the typical configuration with the circles representing spatial data bits. The right-hand side shows a schematic representation of a "bit pattern" in the frequency dimension that could be inscribed within each spatial bit.

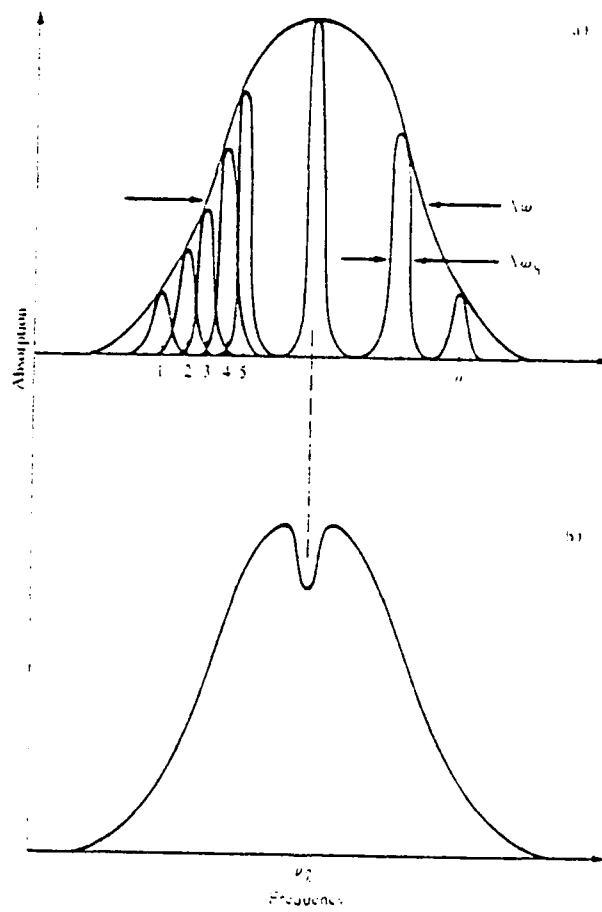


Figure 2.

(a) Symbolic representation of an inhomogeneous absorption line as a superposition of distinguishable sites of the width $\Delta\omega_H$. (b) Line profile during optical saturation or after photochemical reaction with light of frequency ν_l showing burned hole.

PORPHYRIN IN OCTANE AT 1.8° K

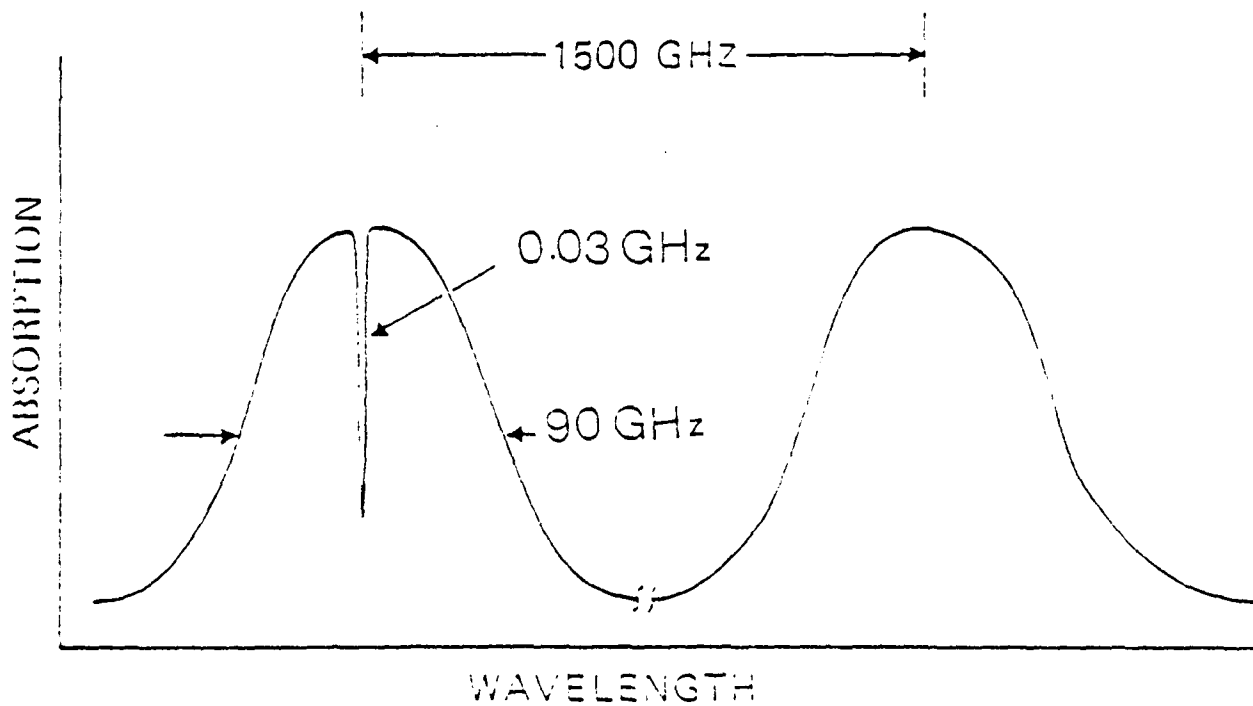
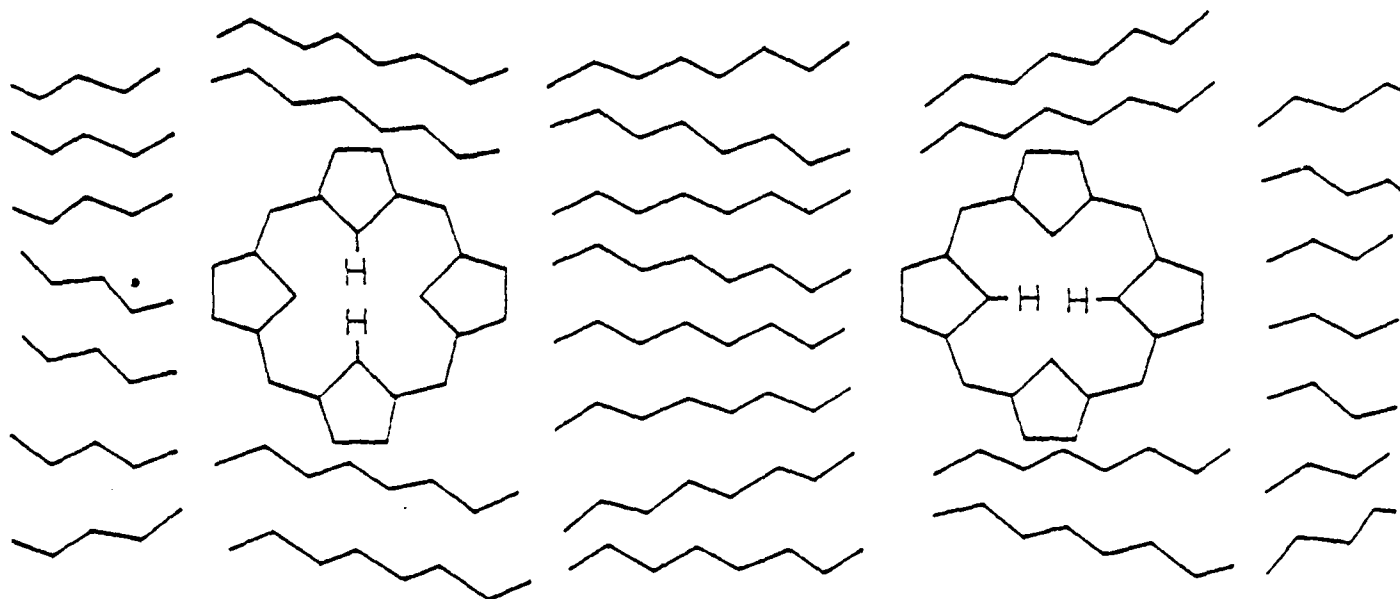


Figure 3. PHB in Porphyrine in Octane.

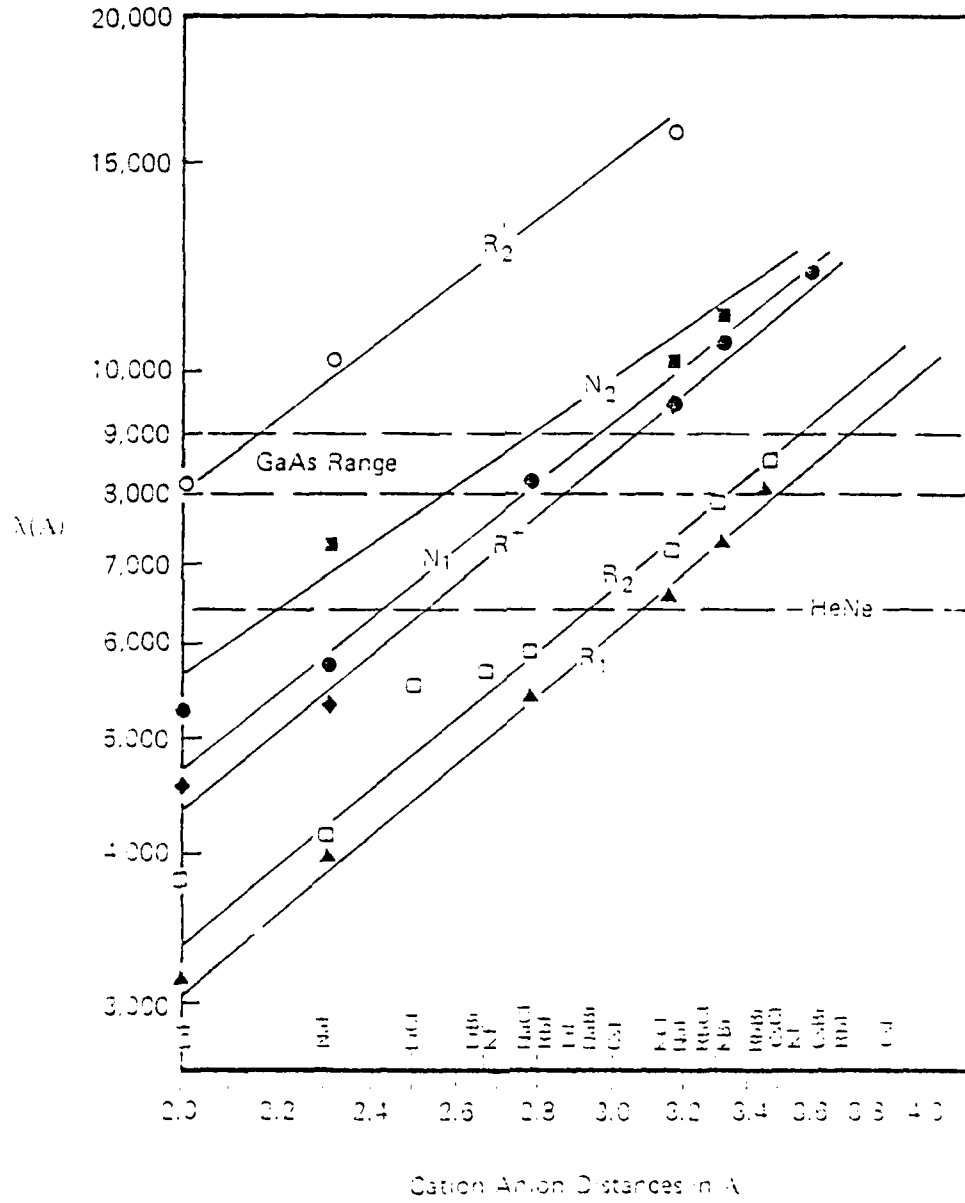


Figure 4. Color Center Absorption

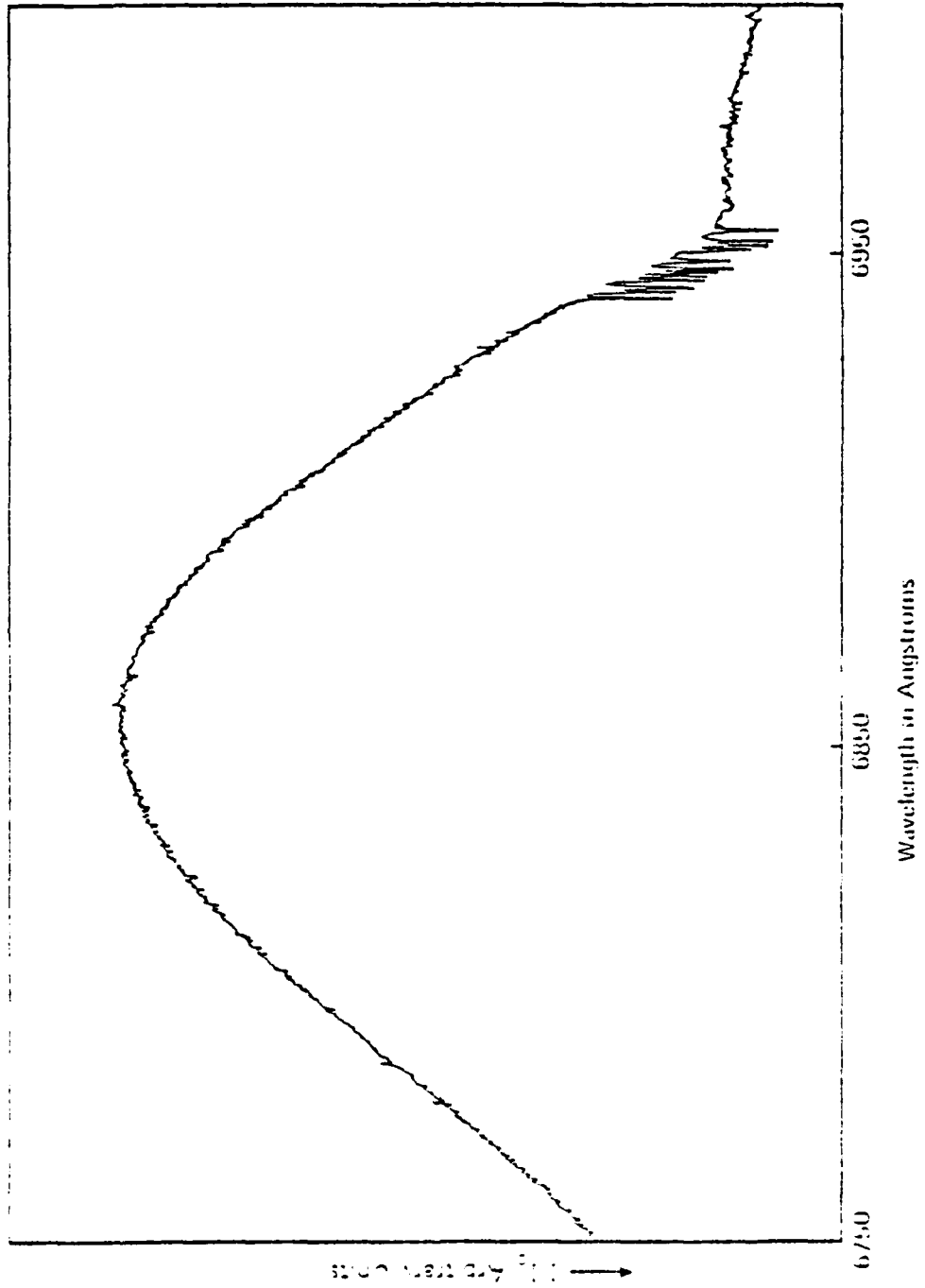


Figure 5. Multiple PIIB in the inhomogeneous O-O absorption band of H₂Pc/PMMA at 4.2K.

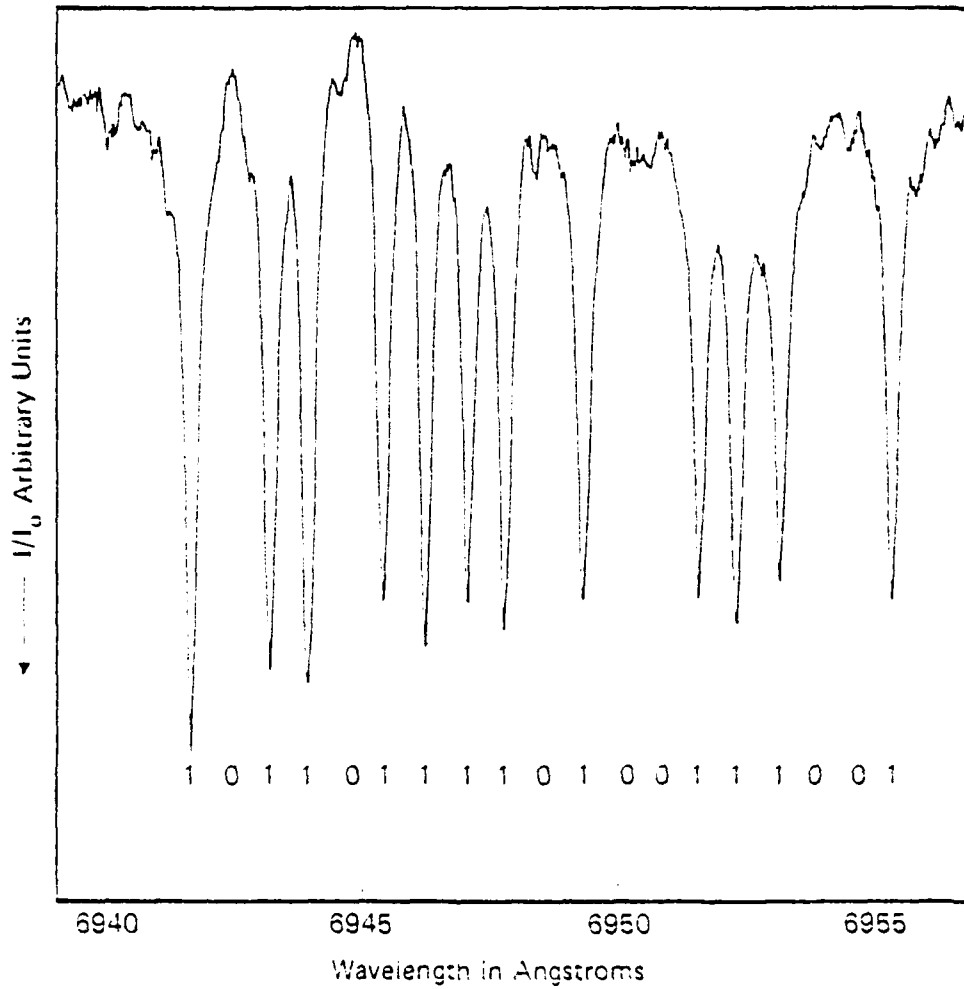


Figure 6.

Same twelve hole spectrum as in Fig. 8 but displayed as an expanded difference - spectrum demonstrating a good signal-to-noise ratio and low background absorption. Labelling with 1's and 0's illustrates a possible 19 bit PHB memory scheme.

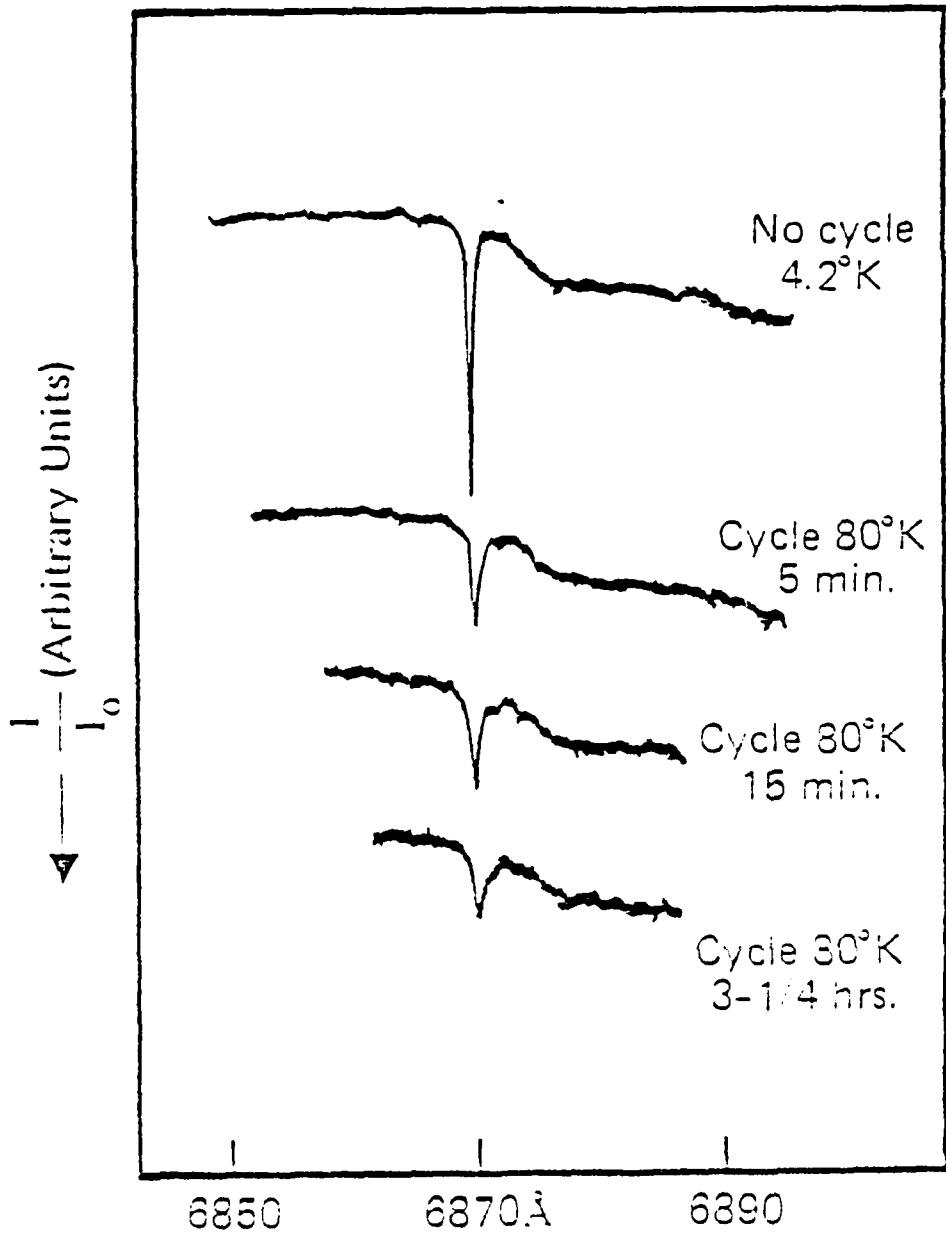


Figure 7.

The effect of temperature cycling to 80K on a photochemical hole burned in H₂Po/PMMA at 4.2K. Note that the ordinate is offset for each spectrum. All spectra were recorded at 4.2K.

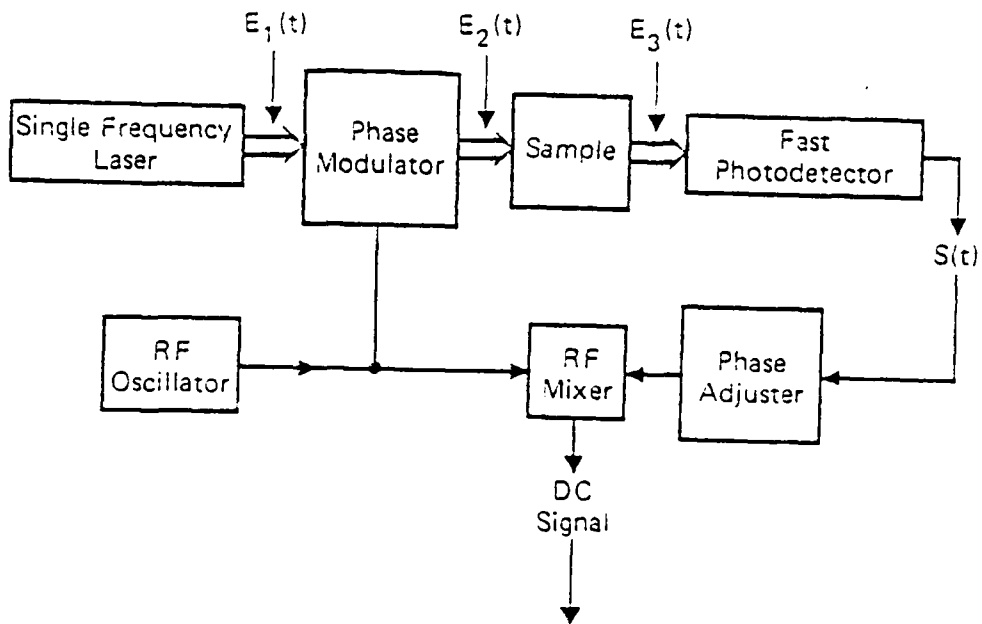


Figure 8. A typical experimental arrangement for FM spectroscopy.

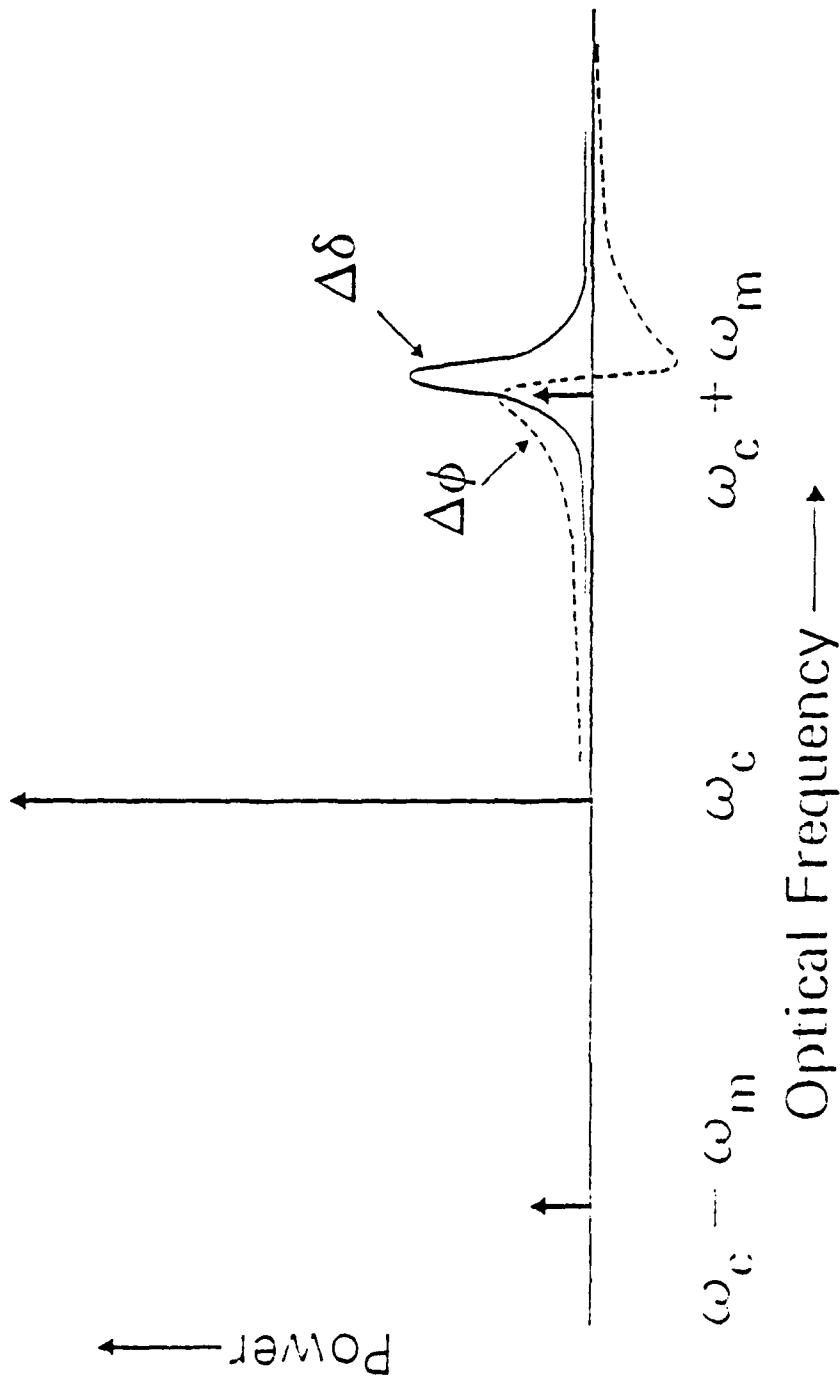
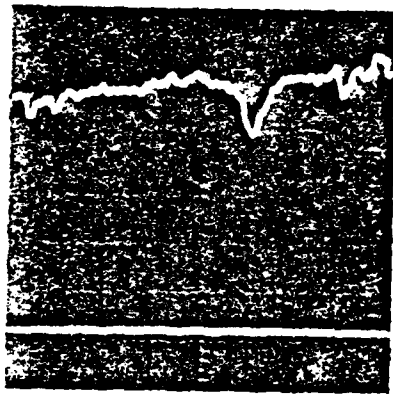
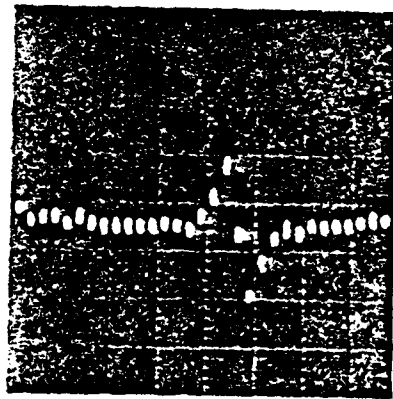


Figure 9. Frequency domain illustration of FM spectroscopy.



(a)



(b)

Figure 10. Experimental demonstration of fast detection of a photochemical hole using FM spectroscopy.

MULTIPLY FM SPECTROSCOPY

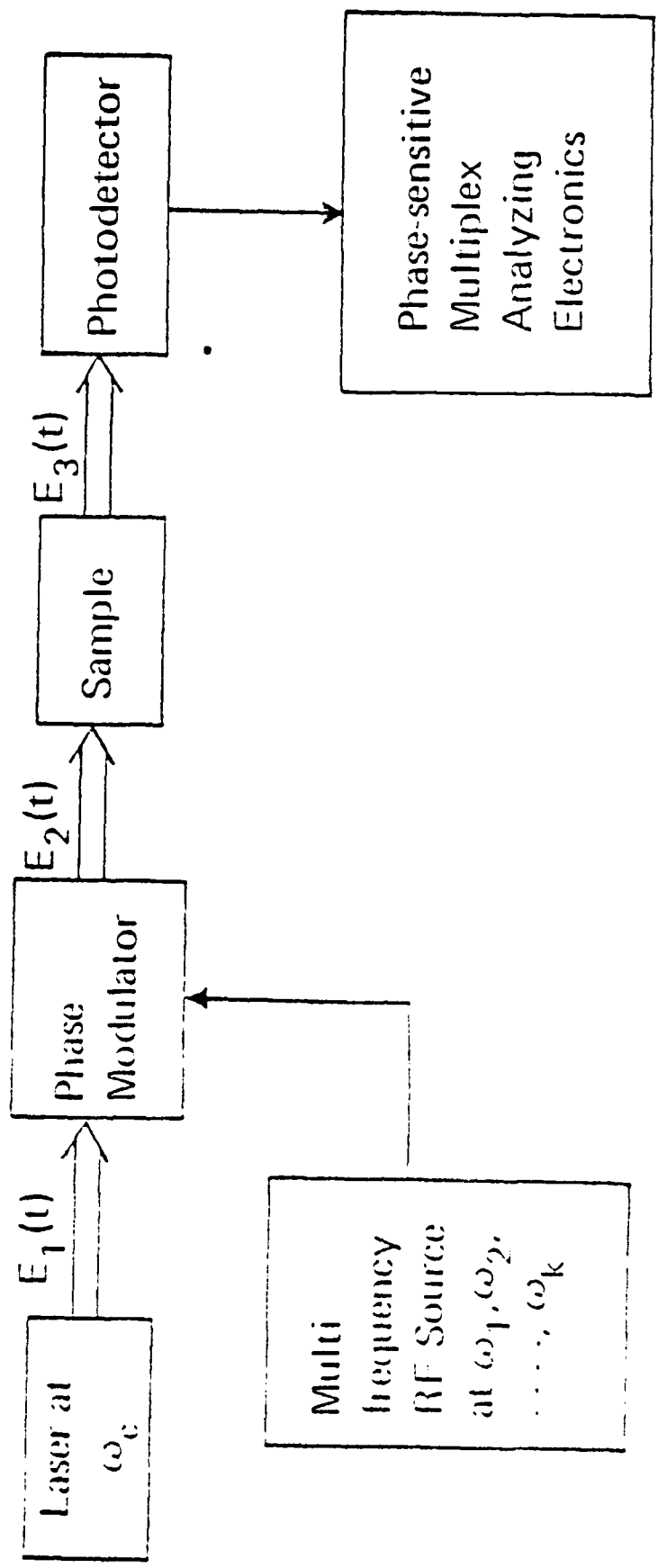


Figure 11. Experimental arrangement for multiplex FM spectroscopy.

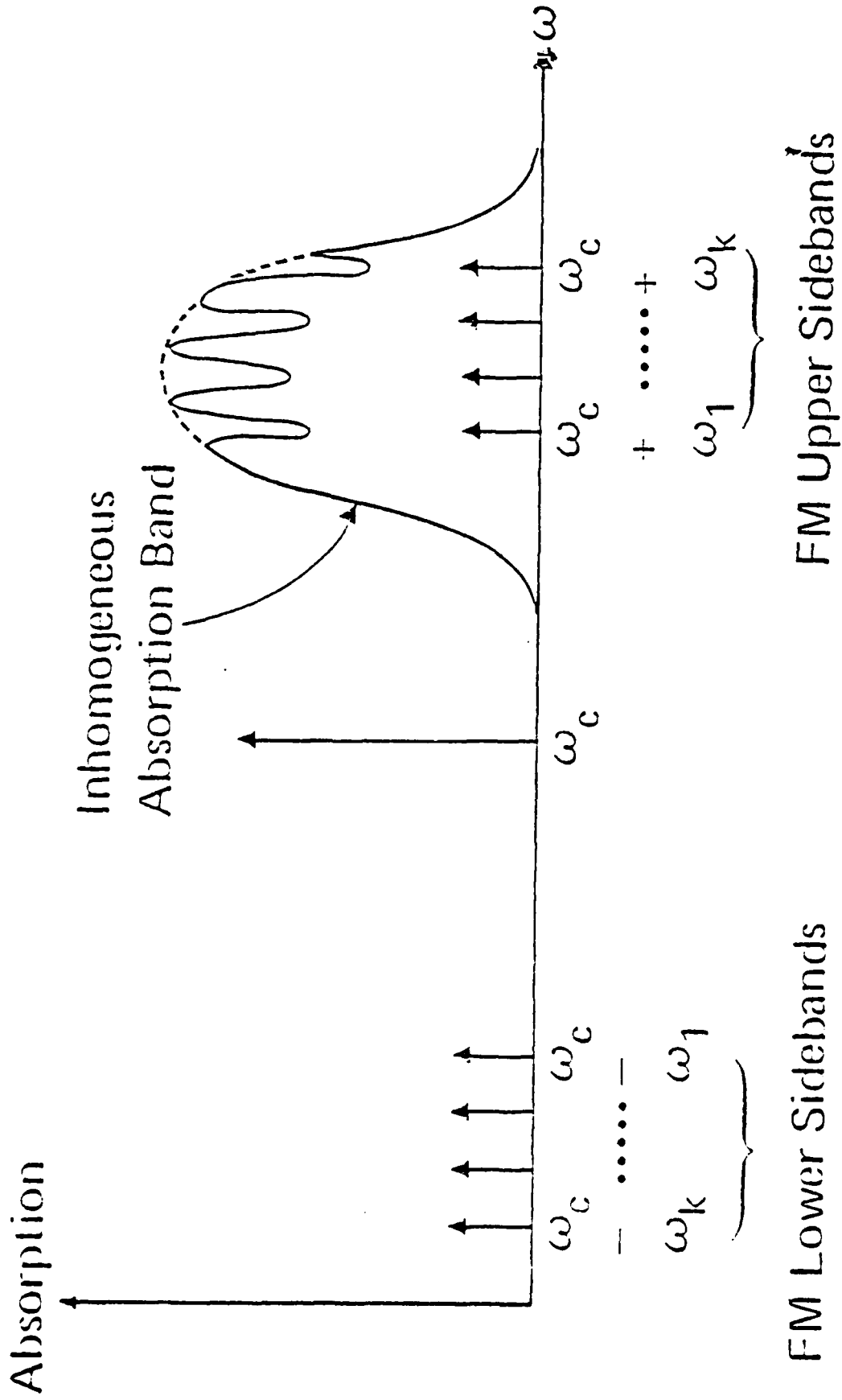
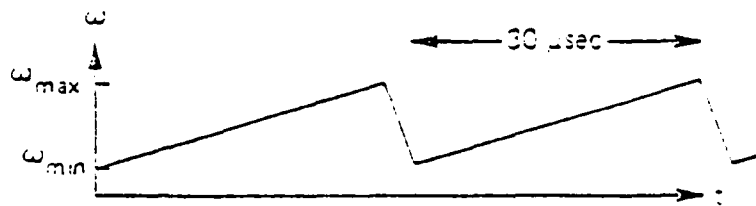


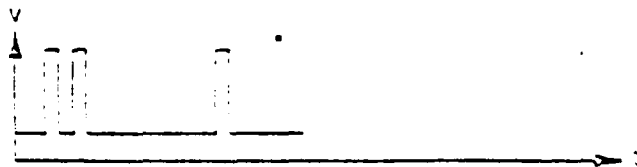
Figure 12 Frequency domain illustration of FM spectroscopy.

• Laser Tuning

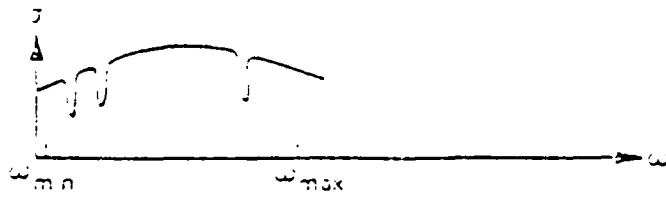


• Writing

Gating Voltage

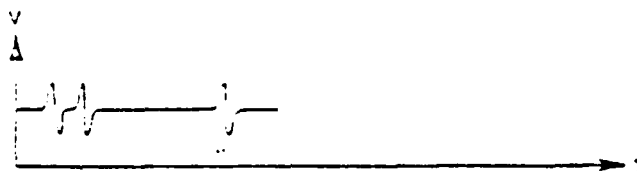


Holes written into absorption line



• Reading

Raw FMI spectroscopy signal



Signal after pulse shaping

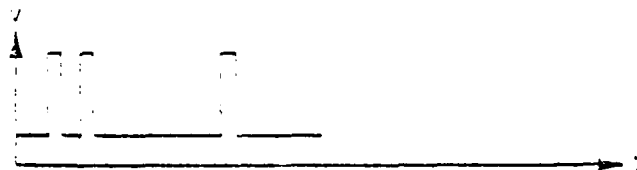


Figure 13.

Reading and Writing Tuning Diagram.

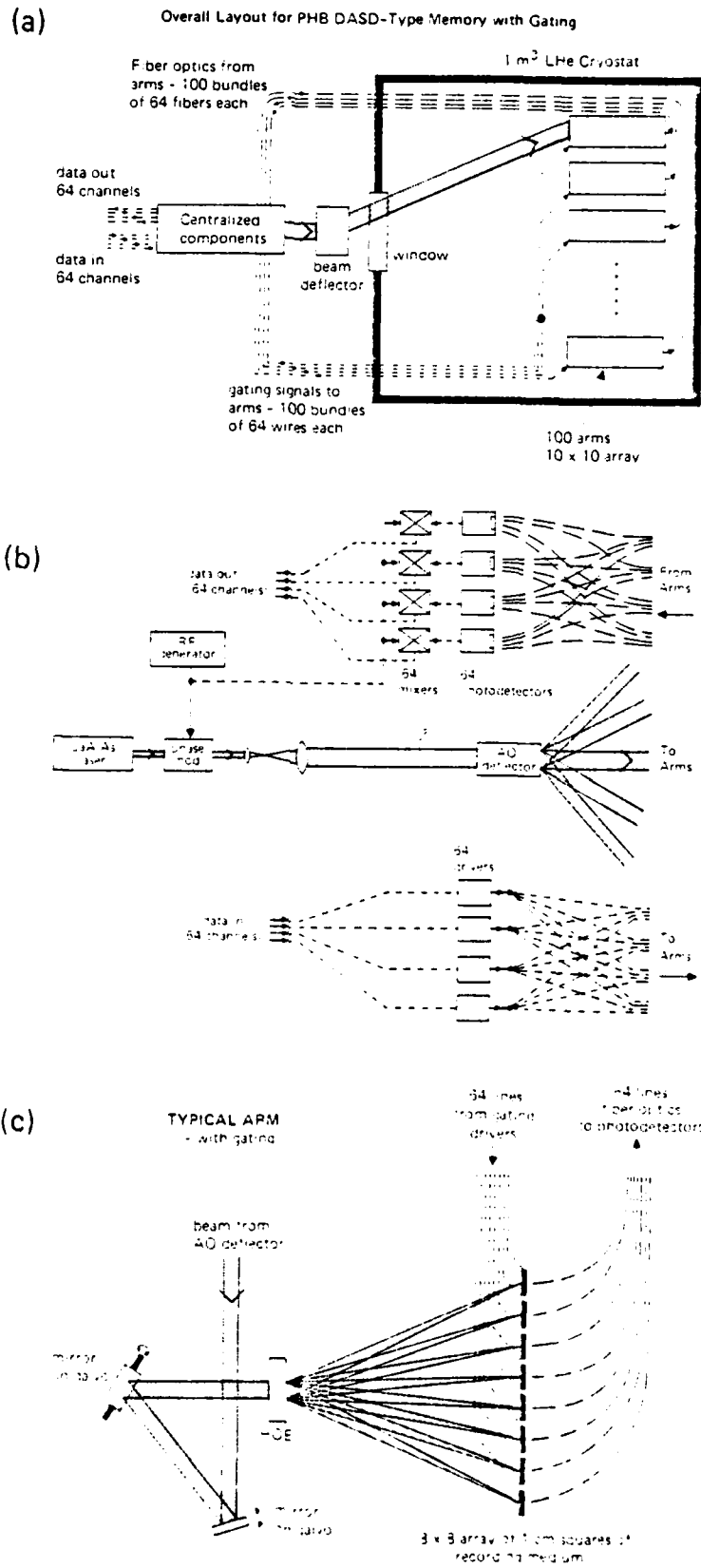
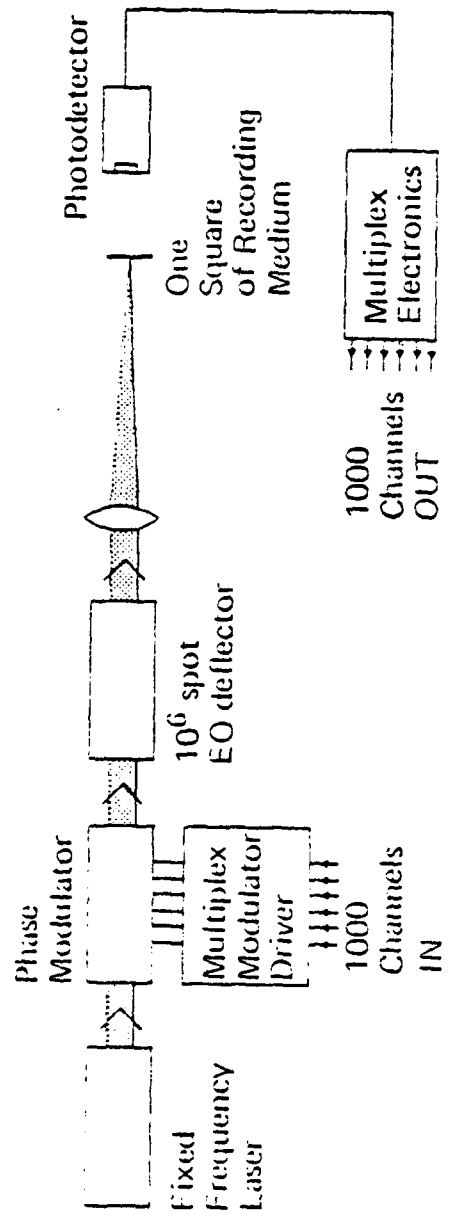


Figure 14. Multiple Arm Memory System.

EO Deflector Plus Multiplex FM Spectroscopy



- 1 μ sec RAT to any 1.0 Kbit page
- 100 nsec to read/write page
- 0.1 gbyte capacity
- 10 gbit/sec burst data rate
- (1 gbit/sec average data rate 1,000,000 I/O per sec)

Figure 15. Memory Configuration.

TECHNICAL REPORT DISTRIBUTION LIST, GEN

	<u>No. Copies</u>		<u>No. Copies</u>
Office of Naval Research Attn: Code 472 800 North Quincy Street Arlington, Virginia 22217	2	U.S. Army Research Office Attn: CRD-AA-IP P.O. Box 1211 Research Triangle Park, N.C. 27709	1
ONR Western Regional Office Attn: Dr. R. J. Marcus 1030 East Green Street Pasadena, California 91106	1	Naval Ocean Systems Center Attn: Mr. Joe McCartney San Diego, California 92152	1
ONR Eastern Regional Office Attn: Dr. L. H. Peebles Building 114, Section D 666 Summer Street Boston, Massachusetts 02210	1	Naval Weapons Center Attn: Dr. A. B. Amster, Chemistry Division China Lake, California 93555	1
Director, Naval Research Laboratory Attn: Code 6100 Washington, D.C. 20390	1	Naval Civil Engineering Laboratory Attn: Dr. R. W. Drisko Port Hueneme, California 93401	1
The Assistant Secretary of the Navy (RE&S) Department of the Navy Room 4E736, Pentagon Washington, D.C. 20350	1	Department of Physics & Chemistry Naval Postgraduate School Monterey, California 93940	1
Commander, Naval Air Systems Command Attn: Code 310C (H. Rosenwasser) Department of the Navy Washington, D.C. 20360	1	Scientific Advisor Commandant of the Marine Corps (Code RD-1) Washington, D.C. 20380	1
Defense Technical Information Center Building 5, Cameron Station Alexandria, Virginia 22314	12	Naval Ship Research and Development Center Attn: Dr. G. Bosmajian, Applied Chemistry Division Annapolis, Maryland 21401	1
Dr. Fred Saalfeld Chemistry Division, Code 6100 Naval Research Laboratory Washington, D.C. 20375	1	Naval Ocean Systems Center Attn: Dr. S. Yamamoto, Marine Sciences Division San Diego, California 91232	1
		Mr. John Boyle Materials Branch Naval Ship Engineering Center Philadelphia, Pennsylvania 19112	1

TECHNICAL REPORT DISTRIBUTION LIST, GEN

	<u>No.</u> <u>Copies</u>
Mr. James Kelley DTNSRDC Code 2803 Annapolis, Maryland 21402	1
Mr. A. M. Anzalone Administrative Librarian PLASTEC/ARRADCOM Bldg 3401 Dover, New Jersey 07801	1

TECHNICAL REPORT DISTRIBUTION LIST, 051A

	<u>No.</u> <u>Copies</u>		<u>No.</u> <u>Copies</u>
Dr. M. A. El-Sayed Department of Chemistry University of California, Los Angeles Los Angeles, California 90024	1	Dr. M. Rauhut Chemical Research Division American Cyanamid Company Bound Brook, New Jersey 08805	1
Dr. E. R. Bernstein Department of Chemistry Colorado State University Fort Collins, Colorado 80521	1	Dr. J. I. Zink Department of Chemistry University of California, Los Angeles Los Angeles, California 90024	1
Dr. C. A. Heller Naval Weapons Center Code 6059 China Lake, California 93555	1		
Dr. J. R. MacDonald Chemistry Division Naval Research Laboratory Code 6110 Washington, D.C. 20375	1	Dr. John Cooper Code 6130 Naval Research Laboratory Washington, D.C. 20375	1
Dr. G. B. Schuster Chemistry Department University of Illinois Urbana, Illinois 61801	1	Dr. William M. Jackson Department of Chemistry Howard University Washington, DC 20059	1
Dr. A. Adamson Department of Chemistry University of Southern California Los Angeles, California 90007	1	Dr. George E. Walraffen Department of Chemistry Howard University Washington, DC 20059	1
Dr. M. S. Wrighton Department of Chemistry Massachusetts Institute of Technology Cambridge, Massachusetts 02139	1	Dr. D. Burland IBM San Jose Research Center 5600 Cottle Road San Jose, California 95143	1
		Dr. A. Paul Schaap Chemistry Department Wayne State University Detroit, Michigan 49202	1

TECHNICAL REPORT DISTRIBUTION LIST, 240

No.
Copies

Mr. Phil Andrews NAVSEA 880 2221 Jefferson Davis Highway Arlington, VA 20360	1
Mr. Romulus Fratillo NAVELEX 613 2511 Jefferson Davis Highway Arlington, VA 20360	1
Mr. B. Zempolich NAVAIR 360B 1411 Jefferson Davis Highway Arlington, VA 2036C	1
Mr. R. Fedorak Naval Air Development Center Warminster, PA 18974	1

END

FILMED

2-83

DTIC